

## Interpretation of Hydrogen Bonding in the Weak and Strong Regions Using Conceptual DFT Descriptors

Alimet Sema Özen,<sup>†</sup> Frank De Proft,<sup>‡</sup> Viktorya Aviyente,<sup>§</sup> and Paul Geerlings<sup>\*‡</sup>

Sabancı University, Orhanlı 34956, Tuzla, İstanbul, Turkey, Eenheid Algemene Chemie, Faculteit Wetenschappen, Vrije Universiteit Brussel, Pleinlaan 2, 1050 Brussels, Belgium, and Department of Chemistry, Boğaziçi University, 34342 Bebek, İstanbul, Turkey

Received: November 24, 2005; In Final Form: March 13, 2006

Hydrogen bonding is among the most fundamental interactions in biology and chemistry, providing an extra stabilization of 1–40 kcal/mol to the molecular systems involved. This wide range of stabilization energy underlines the need for a general and comprehensive theory that will explain the formation of hydrogen bonds. While a simple electrostatic model is adequate to describe the bonding patterns in the weak and moderate hydrogen bond regimes, strong hydrogen bonds, on the other hand, require a more complete theory due to the appearance of covalent interactions. In this study, conceptual DFT tools such as local hardness,  $\eta(\vec{r})$  and local softness,  $s(\vec{r})$ , have been used in order to get an alternative view on solving this hydrogen-bonding puzzle as described by Gilli et al. [*J. Mol. Struct.* **2000**, 552, 1]. A series of both homonuclear and heteronuclear resonance-assisted hydrogen bonds of the types O–H $\cdots$ N, N–H $\cdots$ O, N–H $\cdots$ N, and O–H $\cdots$ O with strength varying from weak to very strong have been studied. First of all,  $\Delta\text{PA}$  and  $\Delta\text{p}K_{\text{a}}$  values were calculated and correlated to the hydrogen bond energy. Then the electrostatic effects were examined as hard–hard interactions accessible through molecular electrostatic potential, natural population analysis (NPA) charge, and local hardness calculations. Finally, secondary soft–soft interaction effects were entered into the picture described by the local softness values, providing insight into the covalent character of the strong hydrogen bonds.

### Introduction

Hydrogen bonding<sup>1</sup> is a unique type of inter- and intramolecular interaction not only for its fundamental role in the vital biological and chemical processes but also for the amount of ambiguity in its operative range. In reality, the spectrum of hydrogen bond strengths extends from 1–4 kcal/mol for weak bonds to 4–15 kcal/mol for moderate bonds and 15–40 kcal/mol for strong bonds.<sup>1</sup> Various models have been developed in order to reveal the mysterious nature of this wide range of interactions. Since hydrogen bonding involves electronegative proton donor and acceptor atoms by definition, the first models were developed on a purely electrostatic basis. Later Gilli et al. would qualify this model as the simple electrostatic model (SEM).<sup>2</sup> By Coulson's<sup>3</sup> introduction of valence-bond (VB) theory into hydrogen bonding, the electrostatic picture was further modulated by delocalizational, repulsive, and dispersive contributions. This idea of partitioning the interaction energy into its components was revisited by Morokuma and others using molecular orbital (MO) theory.<sup>4</sup> According to Morokuma's decomposition method, the hydrogen bond energy can be decomposed into electrostatic, exchange repulsion, polarization, charge transfer, and coupling terms, the first two terms being dominant. The inadequacy of the SEM in describing the resonance-assisted hydrogen bonding (RAHB), among others observed in the O–H $\cdots$ O type of bonds, has led Gilli et al. to focus more on the covalent nature of the hydrogen bonding, which was already suggested occasionally on the basis of both X-ray and neutron diffraction experiments<sup>5</sup> and ab initio and

semiempirical calculations.<sup>6–8</sup> The conclusion stating that “forces determining the hydrogen bond strength are a mixture of both electrostatic and covalent contributions” forms the basis for the electrostatic–covalent hydrogen bond model (ECHBM).<sup>2</sup> According to this model, weak hydrogen bonds are electrostatic in nature. As the strength of the interaction increases, the covalent character of the bond also increases, and very strong hydrogen bonds are actually three-center four-electron covalent bonds. In a beautiful synthesis Gilli et al. finally classified the hydrogen bonds as strong (with subclasses negative charge assisted ((–)CAHB), positive charge assisted, ((+)CHAB), and resonance assisted (RAHB)), moderate (with one subclass of polarization-assisted hydrogen bonds), and weak.<sup>2,9–13</sup> In terms of valence bond theory, the extent of the covalent character of a hydrogen bond is proportional to the mixing of two resonance forms corresponding to the presence or absence of charge transfer:  $-\text{O}-\text{H}\cdots\text{O}=\text{}$  and  $-\text{O}^-\cdots\text{H}-\text{O}^+=$ . Homonuclearity of proton donor and acceptor atoms and symmetry of the molecule then become important for a better mixing. The conditions of minimum proton affinity difference,  $\Delta\text{PA}$ , and of minimum dissociation constant difference,  $\Delta\text{p}K_{\text{a}}$ , for the corresponding protonated forms must be mentioned in this context.<sup>14–17</sup>

In addition to the symmetry and PA matching, it is important to derive general chemical rules that allow predicting the properties of the A–H $\cdots$ B hydrogen bonded system using the information coming from non-interacting A–H and B subsystems. Conceptual density functional theory (DFT),<sup>18–20</sup> which concentrates on the extraction of chemically relevant concepts such as electronegativity,<sup>21</sup> electronic chemical potential,<sup>22</sup> hardness,<sup>23</sup> and softness from DFT, can be the technique of choice to achieve this task. Principles derived within the

<sup>†</sup> Sabancı University.

<sup>‡</sup> Vrije Universiteit Brussel.

<sup>§</sup> Boğaziçi University.

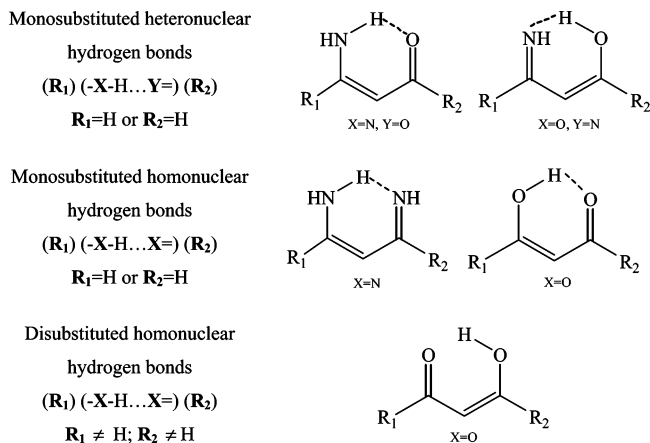


**Figure 1.** Heteronuclear and homonuclear mono- and disubstituted hydrogen bonded structures studied.

framework of conceptual DFT, namely, Sanderson's electronegativity equalization principle<sup>24</sup> and Pearson's hard and soft acids and bases principle<sup>23</sup> and maximum hardness principle,<sup>23</sup> have served for a better understanding of the nature of chemical reactions as well as to predict the intermolecular and intramolecular reactivity trends. Chemical reactivity descriptors have been applied successfully among others by some of the present authors to various types of interactions including acid–base equilibria<sup>25</sup> and a wide variety of organic<sup>26</sup> and inorganic reactions.<sup>27</sup> (For a review see ref 19.)

In a review paper as a part of their systematical and beautiful work on hydrogen bonds, Gilli et al. call the lack of general chemical rules or a unified hydrogen bond theory as *H-bond puzzle*.<sup>2</sup> The aim of the present study is to get an alternative view on solving this puzzle using the tools of conceptual DFT such as local hardness,  $\eta(\vec{r})$ , and local softness,  $s(\vec{r})$ . A series of both homonuclear and heteronuclear resonance-assisted hydrogen bonds of the types O–H...N, N–H...O, N–H...N, and O–H...O with strength varying from weak to very strong have been studied (Figure 1) for this purpose, all of them being of the type intramolecular hydrogen bond, perfectly feasible within the approach if local descriptors are used (vide infra).

## Theoretical Background

**PA/pK<sub>a</sub> matching**<sup>14–17</sup> is a very important concept in the development of the electrostatic–covalent hydrogen bond model. Very strong and symmetrical hydrogen bonds are formed when the difference between the proton affinities of the donor and acceptor atoms approaches zero. A qualitative justification of this trend for ionic hydrogen bonds of the type AH<sup>+</sup>...B was given by Mautner.<sup>14</sup> Partial proton transfer is facilitated, when AH<sup>+</sup> becomes an increasingly more efficient proton donor, i.e., when the proton affinity of neutral A decreases. The partial proton transfer to B is also facilitated when B becomes an increasingly efficient proton acceptor, i.e., when the proton affinity of B increases. The combination of the two factors leads to the inverse relation between  $\Delta\text{PA} = \text{PA}_{\text{donor}} - \text{PA}_{\text{acceptor}}$  and hydrogen bond strength. Also, in the case of highly symmetrical hydrogen bonds,  $\text{PA}_{\text{donor}}$  is very close to  $\text{PA}_{\text{acceptor}}$ , their small difference leading again to the same inverse relation. As a starting procedure,  $\Delta\text{PA}$  and  $\Delta\text{pK}_a$  values have been calculated using the formula below and correlated to the hydrogen bond energy to see if the present systems follow the trends as expected from the literature for PA (now extending to large PA values) and to see if these trends are also reflected in  $\text{pK}_a$  values.

$$\Delta\text{PA} = \text{PA}(\text{X}^-) - \text{PA}(\text{Y}) \quad (1)$$

$$\Delta\text{pK}_a = \text{pK}_a(\text{X}-\text{H}) - \text{pK}_a(\text{H}-\text{Y}^+) \quad (2)$$

In order to investigate the electrostatic component in hydrogen bonding, descriptors suitable for hard–hard interactions have been evaluated. Among these, hardness is a global property describing the resistance to changes in electronic charge,<sup>23</sup>

$$\eta = \left( \frac{\partial\mu}{\partial N} \right)_{\nu(\vec{r})} = \left( \frac{\partial^2 E[N, \nu(\vec{r})]}{\partial N^2} \right)_{\nu(\vec{r})} \quad (3)$$

In eq 3,  $\mu$  is the electronic chemical potential identified as the negative of the electronegativity<sup>21,22</sup> and  $E[N, \nu(\vec{r})]$  is the energy of the system as a function of  $N$ , number of electrons, and  $\nu(\vec{r})$ , the external potential (i.e. due to the nuclei). In the finite difference approximation this is equivalent to

$$\eta \approx I - A \quad (4)$$

where  $I$  and  $A$  are the vertical ionization energy and electron affinity, respectively. For closed shell molecules it can be further approximated as the HOMO–LUMO energy gap. Global softness  $S$  is the inverse of global hardness:

$$S = \frac{1}{\eta} \quad (5)$$

Local hardness, a local counterpart of the global hardness, can be defined as

$$\eta(\vec{r}) = \left( \frac{\delta\mu}{\delta\rho(\vec{r})} \right)_{\nu(\vec{r})} \quad (6)$$

Within the Thomas–Fermi–Dirac (TFD) approach to the DFT and taking into account the exponential falloff of the density in the outer regions of the system, local hardness can be approximated as

$$\eta_{\text{D}}^{\text{TFD}}(\vec{r}) \approx -\frac{1}{2N} V_{\text{el}}(\vec{r}) \quad (7)$$

where  $V_{\text{el}}(\vec{r})$  is the electronic part of the molecular electrostatic potential. The use of the electronic part of the MEP as an approximation to the local hardness has been documented in the literature.<sup>28</sup>

Also the natural population analysis (NPA) charge on the hydrogen atom,  $q_{\text{H}}$ , is a hardness-related descriptor<sup>29,30</sup> and has been used in the literature to gain insight into the acidity of the proton donor. Molecular electrostatic potential (MEP) values can also be used as a substitute of local hardness in the description of hard–hard interactions.

The five classes of hydrogen bonding proposed by Gilli et al.<sup>2,9–13</sup> for the homonuclear O–H...O case indicate the importance of polarizability of acceptor and donor atoms in strong hydrogen bonds. For example, the water dimer represents a weak electrostatic hydrogen bond system with  $\Delta\text{pK}_a = 17.8$ . However, the hydroxyl–water complex,  $[\text{H}-\text{O}\cdots\text{H}\cdots\text{O}-\text{H}]^-$ , which is obtained by the removal of one proton from the water dimer, is a (–)CAHB system with strong and symmetric interactions with  $\Delta\text{pK}_a = 0$ . In the same manner, the addition of one proton to the dimer transforms the water dimer in the hydronium–water complex,  $[\text{H}_2\text{O}\cdots\text{H}\cdots\text{OH}_2]^+$ , which is of the (+)CAHB type accompanied by a reduction to zero in  $\Delta\text{pK}_a$ .<sup>13</sup> In summary, X–H...Y is a strong hydrogen bond system if H is in the form of H<sup>+</sup> or X, Y are in the form of either X<sup>–</sup> or Y<sup>–</sup>.

Therefore, in addition to hard–hard interactions, the charged H may stabilize the system by polarizing A and B and local softness values can be employed to probe the extent of the polarization of A and B. Therefore, they might provide a measure for covalency.

The local softness  $s(\vec{r})$  describes the local response of the electron density  $\rho(\vec{r})$  upon a change in the electronic chemical potential:<sup>18–20</sup>

$$s(\vec{r}) = \left( \frac{\partial \rho(\vec{r})}{\partial \mu} \right)_{v(\vec{r})} \quad (8)$$

This local quantity can be coupled to its global counterpart  $S$  via the Fukui function  $f(\vec{r})$ . This descriptor “measures how sensitive a system’s chemical potential is to an external perturbation at a particular point”.<sup>18</sup> It also gives information about local change in the electron density of an atom or molecule upon changing the total number of electrons.<sup>18–20,31</sup>

$$f(\vec{r}) = \left( \frac{\delta \mu}{\delta v(\vec{r})} \right)_N = \left( \frac{\partial \rho(\vec{r})}{\partial N} \right)_{v(\vec{r})} \quad (9)$$

The two local properties  $s(\vec{r})$  and  $f(\vec{r})$  are related to each other through the global softness,  $S$ :

$$s(\vec{r}) = f(\vec{r})S \quad (10)$$

Since, however,  $\partial \rho(\vec{r})/\partial N$  is a discontinuous function of  $N$ , it will have one value from the right, one from the left, and an average at some integral value of  $N$ :

$$f^+(\vec{r}) = [\partial \rho(\vec{r})/\partial N]^+_{v(\vec{r})} \quad (\text{when } N \text{ goes from } N_0 \text{ to } N_0 + \delta) \quad (11a)$$

$$f^-(\vec{r}) = [\partial \rho(\vec{r})/\partial N]^-_{v(\vec{r})} \quad (\text{when } N \text{ goes from } N_0 - \delta \text{ to } N_0) \quad (11b)$$

$$f^0(\vec{r}) = \frac{1}{2}[f^+(\vec{r}) + f^-(\vec{r})]^0 \quad (\text{average}) \quad (11c)$$

Here  $f^+(\vec{r})$  is the reactivity index for a nucleophilic attack,  $f^-(\vec{r})$  for an electrophilic attack, and  $f^0(\vec{r})$  for a radical attack. A condensed form of these functions employs the atomic populations  $q_k$ , within a finite difference approximation:

$$f^+ = q_k(N + 1) - q_k(N) \quad (12a)$$

$$f^- = q_k(N) - q_k(N - 1) \quad (12b)$$

$$f^0 = \frac{1}{2}[q_k(N + 1) - q_k(N - 1)] \quad (12c)$$

### Computational Methodology

In the present study, the intramolecular hydrogen bonded structures and types of substituents have been selected in such a way as to be similar to the ones investigated extensively by Gilli et al.,<sup>11</sup> in order to allow a parallel discussion and comparison between the two studies (Figure 1). Intramolecular hydrogen bonding energies ( $E_{\text{HB}}$ ) have been calculated as the interaction energy between the bonded and nonbonded conformers. Non hydrogen bonded conformers have been selected systematically in the same manner mentioned in the literature leading to a hydrogen bond energy equation

$$\Delta E_{\text{HB}}(\text{cT}) = E(\text{open cT}) - E(\text{closed cC}) \quad (13)$$

where the cT and cC geometries are shown in Figure 2. On the

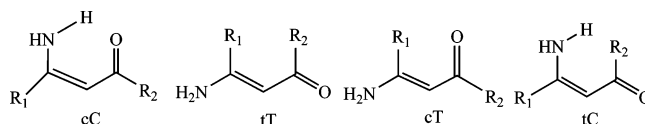


**Figure 2.** Hydrogen bonded and non hydrogen bonded conformers.

other hand, there were some cases where this representation caused new hydrogen bonding patterns related to the substituents. In such special cases either the tT conformers of Figure 2 have been used or new conformers have been obtained by simply rotating the H atom. Also, there were cases where steric effects could have been effective for more crowded substituents. In these, especially disubstituted, cases, either the H atom subject to hydrogen bonding has been rotated or, if this rotation causes the formation of a new hydrogen bond, the  $R_1$ – $R_2$  dihedral angle in the tT conformation and the  $R_1$ –O dihedral angle in the cT conformation have been slightly distorted from planarity to lessen the steric effects. The effect of the relative energies of the different conformers on the calculation of the hydrogen bonding energy has been found not to exceed 1–1.5 kcal/mol in the monosubstituted benchmarks. Due to a possible loss of planarity, hence degree of electron delocalization, the hydrogen bond energies presented here can be considered as the upper limit in these exceptional cases.

Enthalpy contributions have been taken into account during the calculation of hydrogen bond energies ( $E_{\text{HB}}$ ) used for PA/ $pK_a$  matching analysis. However, only electronic energies without zero-point correction have been employed (as reactivity descriptors in general only refer to purely electronic energies) for determining the correlations between the hydrogen bond energy and the reactivity descriptors such as qH, MEP,  $\eta(\vec{r})$ , and  $s(\vec{r})$ . Nevertheless, through normal mode analysis, all of the structures have been confirmed to be in their ground state without imaginary frequencies.

In extensive benchmark studies on low-barrier hydrogen bonds, McAllister et al.<sup>32</sup> have shown that density functional methods (BLYP and B3LYP) perform almost identically to other correlated ab initio methods such as MPn, QCISD, and CCSD. They have also concluded that 6-31+G(d,p) is an excellent and sufficient basis set for further studies of these types of systems. Therefore, all of the calculations in the present study have been performed at the B3LYP/6-31+G(d,p) level of theory using the Gaussian 03 program.<sup>33</sup> Atomic charges have been calculated as NPA charges.

### Results and Discussion

Tables 1–4 show the hydrogen bond electronic energy values with and without zero-point energy corrections and the corresponding enthalpy and free energy values. In this study, all of the calculations related to the PA and  $pK_a$  values and reactivity descriptors have been performed on the non hydrogen bonded or isolated forms of the acceptor and donor atoms, i.e., when donor and acceptor atoms “do not see each other”. It is necessary to note that when  $R_2 = \text{NH}_2$  and OH in the heteronuclear monosubstituted O–H $\cdots$ N case and when  $R_1 = \text{F}$  in the homonuclear monosubstituted O–H $\cdots$ O case, it was not possible to obtain the optimized geometries in the closed cC form since the proton simply preferred to pass to the acceptor atom rather than staying on the donor atom. This can be explained by the presence of strong electron donor substituents ( $\text{NH}_2$  and OH) on the acceptor side making the acceptor more electron-rich and attracting the proton in the former case and by the presence of a strong electron-withdrawing substituent (F) on

**TABLE 1: Hydrogen Bond Energies and  $\Delta PA$  and  $\Delta pK_a$  Values between the Acceptor Y and Donor X Atoms for the Monosubstituted Heteronuclear Compounds<sup>a</sup>**

(R <sub>1</sub> )(-X-H...Y=)(R <sub>2</sub> )							
R <sub>1</sub>	R <sub>2</sub>	$\Delta E$	$\Delta(E + ZPE)$	$\Delta H$	$\Delta G$	$\Delta PA$	$\Delta pK_a$
X = N, Y = O							
H	H	4.42	3.50	4.12	2.03	125.57	129.44
CH <sub>3</sub>	H	7.98	5.67	6.36	4.80		
H	NH <sub>2</sub>	7.78	6.84	7.41	6.42	129.17	129.55
H	NO <sub>2</sub>	5.85	2.00	2.50	1.41	134.40	134.78
H	OH	4.01	1.51	1.96	1.03	136.88	138.48
Cl	H	8.62	8.24	8.50	7.83	115.62	114.85
F	H	8.54	8.18	8.41	7.85	119.89	120.28
NH <sub>2</sub>	H	7.64	7.46	7.61	7.16	114.32	114.26
NO <sub>2</sub>	H	7.99	7.32	7.71	6.70	142.87	143.46
OH	H	8.29	7.80	8.13	7.28	121.35	121.91
X = O, Y = N							
H	H	6.35	6.46	6.47	6.57	83.16	105.69
CH <sub>3</sub>	H	6.50	6.22	6.20	6.05		
H	NH <sub>2</sub>					82.25	81.54
H	NO <sub>2</sub>	13.35	13.60	14.04	13.03	95.72	94.83
H	OH					83.16	83.96
Cl	H	10.37	9.72	10.22	8.91		
F	H	10.16	9.49	9.96	8.83	112.05	112.04
NH <sub>2</sub>	H	12.80	12.56	13.02	11.89	98.29	98.78
NO <sub>2</sub>	H	8.62	8.12	8.50	7.52	112.76	112.69
OH	H	12.23	11.68	11.68	11.62	104.34	102.42

<sup>a</sup> All values are in kcal/mol.  $E$  = electronic energy,  $E + ZPE$  = electronic energy with zero-point energy correction,  $H$  = enthalpy,  $G$  = free energy.

**TABLE 2: Hydrogen Bond Energies and  $\Delta PA$  and  $\Delta pK_a$  Values between the Acceptor N and Donor N Atoms for the Monosubstituted Homonuclear Nitrogen Compounds<sup>a</sup>**

(R <sub>1</sub> )(-N-H...N=)(R <sub>2</sub> )							
R <sub>1</sub>	R <sub>2</sub>	$\Delta E$	$\Delta(E + ZPE)$	$\Delta H$	$\Delta G$	$\Delta PA$	$\Delta pK_a$
H	H	7.61	7.23	7.50	6.86	113.56	114.01
H	H	6.98	6.41	6.80	5.91	114.96	115.91
CH <sub>3</sub>	H	7.10	6.78	7.05	6.34	108.02	107.97
H	NH <sub>2</sub>	6.48	6.24	6.41	5.99	108.76	109.14
H	NO <sub>2</sub>	5.72	4.97	5.45	4.23	118.64	119.84
H	OH	5.82	5.45	5.68	5.14	119.66	120.01
Cl	H	8.77	8.68	8.85	8.42		
F	H	8.81	8.71	8.84	8.63	101.72	101.78
NH <sub>2</sub>	H	7.38	7.21	7.40	6.87	98.73	98.38
NO <sub>2</sub>	H	8.04	7.68	7.96	7.23	107.50	107.49
OH	H	8.35	8.08	8.36	7.47	105.91	106.99
H	Cl	5.80	5.11	5.57	4.39		
H	F	5.77	5.12	5.52	4.53	121.06	121.90
H	CH <sub>3</sub>	6.16	5.92	6.66	5.00		

<sup>a</sup> All values are in kcal/mol.  $E$  = electronic energy,  $E + ZPE$  = electronic energy with zero-point energy correction,  $H$  = enthalpy,  $G$  = free energy.

the donor side making the donor electron-poor and repelling the proton toward the acceptor for the latter. This is in accordance with Gilli's comments on the relationship between the hydrogen bond strength and electron-donating and -withdrawing substituents on the acceptor and donor sites.<sup>12</sup>

The first two rows in Tables 2 and 3 correspond to the energies calculated using different non hydrogen bonded conformers (tC and cT, respectively) of the same hydrogen bonded molecule. The difference in hydrogen bond energies is quite small in both cases.

**Proton Affinity (PA) and Dissociation Constant ( $pK_a$ ) Perspective on Hydrogen Bond Strength.** The proton affinity has been calculated as the negative enthalpy change associated with the gas-phase protonation reaction  $X^- + H^+ = XH$  of the donor and  $Y + H = YH^+$  of the acceptor atoms for the

**TABLE 3: Hydrogen Bond Energies and  $\Delta PA$  and  $\Delta pK_a$  Values between the Acceptor O and Donor O Atoms for the Monosubstituted Homonuclear Oxygen Compounds<sup>a</sup>**

(R <sub>1</sub> )(-O-H...O=)(R <sub>2</sub> )							
R <sub>1</sub>	R <sub>2</sub>	$\Delta E$	$\Delta(E + ZPE)$	$\Delta H$	$\Delta G$	$\Delta PA$	$\Delta pK_a$
H	H	10.18	9.64	10.02	9.16	125.01	125.23
H	H	8.87	8.42	8.81	7.96	121.78	122.17
CH <sub>3</sub>	H	10.97	10.56	10.89	10.16	121.04	120.04
H	NH <sub>2</sub>	9.47	8.90	9.38	7.88	121.80	124.32
H	NO <sub>2</sub>	5.52	5.07	5.36	4.71	132.76	132.53
H	OH	7.45	6.97	7.29	6.57	132.24	131.95
Cl	H	12.81	13.03	13.41	12.54		
F	H					106.46	106.49
NH <sub>2</sub>	H	13.91	14.11	14.45	13.78	104.76	105.65
NO <sub>2</sub>	H	11.47	11.06	11.47	10.51	109.60	108.79
OH	H	12.97	12.93	13.37	12.36	109.27	107.40
H	Cl	6.91	6.34	6.70	5.90		
H	F	6.94	6.34	6.68	5.92	127.85	128.25
H	CH <sub>3</sub>	10.14	9.67	10.68	7.45	115.76	118.61
CF <sub>3</sub>	H	10.80	10.30	10.68	9.85	119.36	118.29
H	N(CH <sub>3</sub> ) <sub>2</sub>	14.79	14.24	14.58	14.06	105.97	107.81

<sup>a</sup> All values are in kcal/mol.  $E$  = electronic energy,  $E + ZPE$  = electronic energy with zero-point energy correction,  $H$  = enthalpy,  $G$  = free energy.

**TABLE 4: Hydrogen Bond Energies and  $\Delta PA$  and  $\Delta pK_a$  Values between the Acceptor and Donor Atoms for the Disubstituted Homonuclear Oxygen Compounds<sup>a</sup>**

(R <sub>1</sub> )(-O-H...O=)(R <sub>2</sub> )							
R <sub>1</sub>	R <sub>2</sub>	$\Delta E$	$\Delta(E + ZPE)$	$\Delta H$	$\Delta G$	$\Delta PA$	$\Delta pK_a$
NH <sub>2</sub>	NO <sub>2</sub>	15.53	15.18	15.48	14.69	96.95	97.70
NO <sub>2</sub>	Cl	12.60	12.13	12.53	11.61	104.23	104.43
NO <sub>2</sub>	CH <sub>3</sub>	16.88	16.67	17.07	16.38	101.33	101.33
NO <sub>2</sub>	NH <sub>2</sub>	18.25	17.61	18.29	16.14	102.02	104.50
NO <sub>2</sub>	OH	16.83	16.26	16.75	15.55	100.26	100.86
NO <sub>2</sub>	OCH <sub>3</sub>	17.78	17.42	17.86	16.71	94.66	95.22
NO <sub>2</sub>	NHCOCH <sub>3</sub>	17.95	17.50	17.99	16.45	81.77	82.85
COCl	NH <sub>2</sub>	16.30	15.65	16.12	15.22	108.45	109.00
COCl	OCH <sub>3</sub>	16.12	15.57	15.96	15.15	100.79	100.60
COCl	OH	20.60	19.70	20.15	19.31	106.24	106.24
COCl	CH <sub>3</sub>	15.29	14.88	15.21	14.96	106.60	106.46
COCl	N(CH <sub>3</sub> ) <sub>2</sub>	17.15	16.69	17.07	16.36	101.23	102.71
CF <sub>3</sub>	NH <sub>2</sub>	18.52	18.15	18.42	17.63	111.66	112.51
CF <sub>3</sub>	OH	17.44	16.88	16.62	17.73	110.69	107.57
CF <sub>3</sub>	N(CH <sub>3</sub> ) <sub>2</sub>	17.82	17.29	17.59	17.48	104.80	106.39
CN	N(CH <sub>3</sub> ) <sub>2</sub>	15.47	15.05	15.43	13.93	102.21	104.24
N(CH <sub>3</sub> ) <sub>2</sub>	F	16.49	16.18	16.27	16.74	104.03	103.31
F	NH <sub>2</sub>	15.41	15.24	15.83	14.20	101.00	102.99

<sup>a</sup> All values are in kcal/mol.  $E$  = electronic energy,  $E + ZPE$  = electronic energy with zero-point energy correction,  $H$  = enthalpy,  $G$  = free energy.

molecular structures with the general representation of (R<sub>1</sub>)(-X-H...Y=)(R<sub>2</sub>).  $pK_a$  values have been obtained by means of the change in free energy for the dissociation reactions  $X-H = X^- + H^+$  and  $YH^+ = Y + H^+$  within the same class of compounds. In Tables 1–4, the  $\Delta PA$  and  $\Delta pK_a$  values between the acceptor and donor atoms together with the hydrogen bonding energies have been tabulated. It should be noted that, in these tables, some values of  $\Delta PA$  and  $\Delta pK_a$  are missing for certain CH<sub>3</sub> and Cl substitutions due to some optimization problems. In the case of Cl, deprotonation of the donor atom (structures related to X<sup>-</sup>) caused the cleavage of the C–Cl bond, increasing the interatomic distance up to 1.985 Å. In some cases of CH<sub>3</sub> it was not possible to get rid of the imaginary frequencies corresponding to the rotations of the CH<sub>3</sub> group for the X<sup>-</sup> and YH<sup>+</sup> forms. There have been several experimental and computational studies in the literature, describing the increase in hydrogen bond energy with a decrease in  $\Delta PA$  or  $\Delta pK_a$ . In this work, we are exploring the correlation in a broader range of

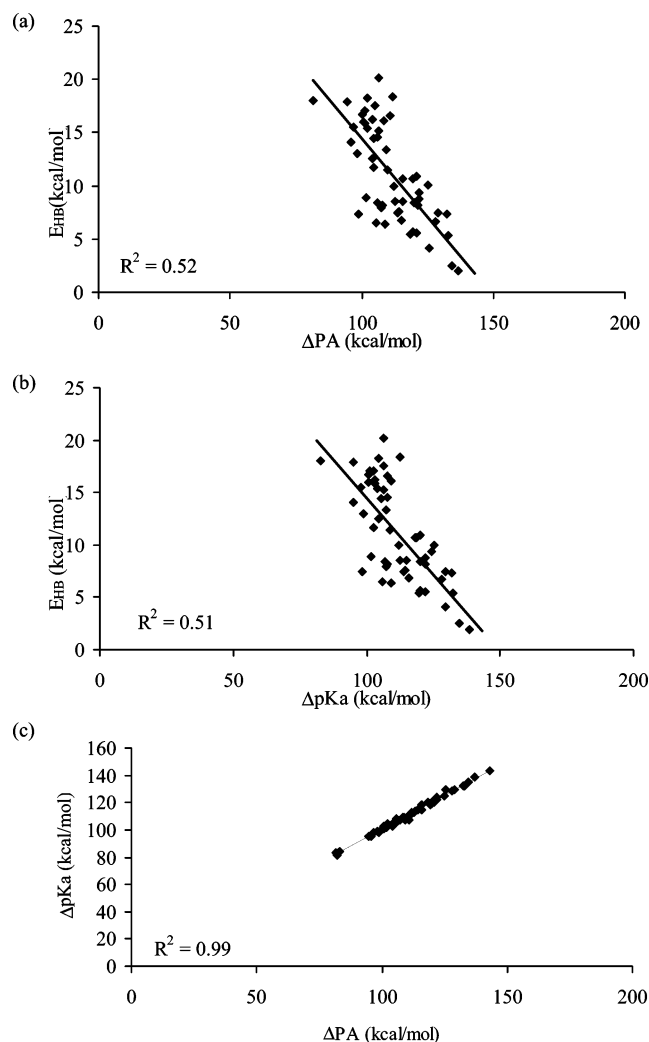


**Figure 3.**  $E_{HB}$  (kcal/mol) versus (a)  $\Delta PA$  (kcal/mol) and (b)  $\Delta pK_a$  for 56 structures in all hydrogen bonding regimes. The correlation for  $\Delta PA$  versus  $\Delta pK_a$  is shown in panel c.

structures of both homonuclear and heteronuclear types, including strong, moderate, and weak hydrogen bonding regimes with a special interest in the resonance-assisted hydrogen bond (RAHB) situations of intramolecular hydrogen bonding.

The effect of PA and  $pK_a$  matching between acceptor and donor atoms on the hydrogen bonding strength can be seen in Figure 3a and Figure 3b, respectively. In addition, Figure 3c represents the perfect correlation between  $\Delta PA$  and  $\Delta pK_a$  values within themselves. The overall correlation has been quite moderate when the whole range of structures has been considered ( $R^2 = 0.52$  and  $0.51$  for  $\Delta PA$  and  $\Delta pK_a$  cases, respectively). But, when they have been classified as homonuclear and heteronuclear and also as  $N-H\cdots N$  and  $O-H\cdots O$  types, much better correlations have been obtained. This situation is in accordance with the findings of Chandra<sup>17</sup> and also the others, stating that the correlations between the hydrogen bonding energies and  $\Delta PA$  were valuable only for closely related systems in the case of intermolecular hydrogen bonded complexes. That is indeed the case in our intramolecular hydrogen bonded systems. In the case of heteronuclear compounds ( $N-H\cdots O$  and  $N\cdots H-O$ ) the correlation was improved to the value of 0.78. Homonuclear  $N-H\cdots N$  compounds in the weak hydrogen bonding regime showed the worst correlation ( $R^2 = 0.65$ ). Their monosubstituted  $O-H\cdots O$  counterparts in the weak–moderate hydrogen bonding regime, however, yield a good correlation coefficient ( $R^2 = 0.90$ ) whereas this value drops to 0.72 by the

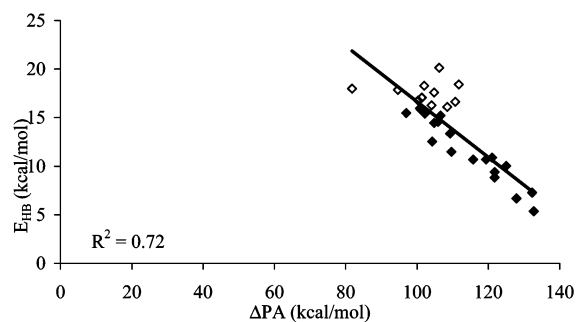


**Figure 4.**  $E_{HB}$  (kcal/mol) versus  $\Delta PA$  (kcal/mol) for mono- and disubstituted  $O-H\cdots O$  type of hydrogen bonds ( $R^2 = 0.91$  when only  $E_{HB} < 16$  kcal/mol points are considered).

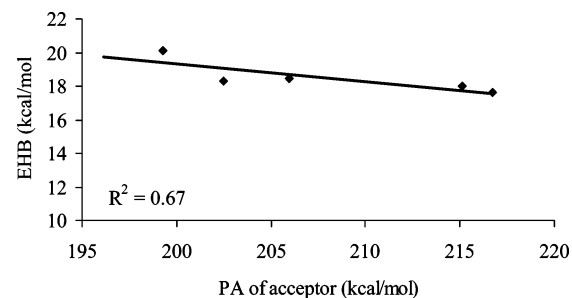


**Figure 5.**  $E_{HB}$  (kcal/mol) versus PA (kcal/mol) of acceptor for hydrogen bonds where  $E_{HB} > 16$  kcal/mol.

introduction of disubstituted, strong hydrogen bond structures. Figure 4 shows the hydrogen bonding energy as a function of  $\Delta PA$  for mono- and disubstituted  $O-H\cdots O$  types of compounds in the weak–moderate–strong hydrogen bonding regime. As it can be seen, there is a deviation from linearity in the region of strong hydrogen bonds. Excluding these points above 16 kcal/mol on the graph leads to an improvement of the correlation to 0.91. In order to get a better understanding of this behavior, the effects of the donor's PA and acceptor's PA on the hydrogen bond energy have been examined separately for all of the regimes. It has been observed that the PA of the acceptor was the dominating parameter for this particular type of interaction. In the weak and moderate regimes, hydrogen bonding energy has been increasing with increasing values of the acceptor proton affinity, with mostly moderate correlations ( $R^2 \approx 0.61$ – $0.95$ ), whereas there was no specific correlation in terms of the donor proton affinity. On the other hand, in the strong hydrogen bonding regime, neither the acceptor's nor the donor's PA values have been correlated to the hydrogen bond energies and there even was observed a plateau in the former case with a tendency to incline in the opposite direction to the expectations. As it can be seen in Figure 5, the hydrogen bond energy increases as the PA of the acceptor decreases when  $E_{HB} > 16$  kcal/mol. This trend might be surprising at first sight but can also be the first hint for the presence of other factors contributing to the hydrogen bond energy other than electrostatics in the strong regime.

Chandra et al. discerned a greater importance of the proton donor on the hydrogen bonding energy for the series of intermolecular complexes they studied.<sup>17</sup> In their study the best correlations were obtained when weighting the PA of the proton donor and the proton acceptor by 1.5 and 1, respectively. We have also observed a similar situation in our systems for the overall correlation. However, when the individual homonuclear and heteronuclear systems have been considered, the particular subcorrelations have turned out to be much poorer and the improvement in overall correlation is only artificial. According to our data, proton affinity of the donor is not the dominant

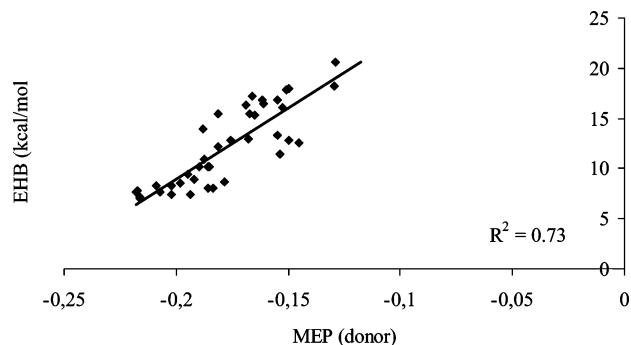


**Figure 6.** Hydrogen bond energy ( $E_{\text{HB}}$ ) versus MEP of donor atom in the moderate and strong hydrogen bond region for moderate and strong types of hydrogen bonding (when  $E_{\text{HB}} > 7$  kcal/mol).

parameter and increasing its contribution will disturb the correlations with hydrogen bond energy for the subsystems. Therefore, a nonbiased equal weighting of donor and acceptor proton affinities must be preferred even though they might not always give the condition of best overall correlation.

**Hardness Role.** NPA charges ( $q_{\text{H}}$ ) have been extracted, as an indicator of hardness of the hydrogen atom subject to the hydrogen bond interaction, both in the homonuclear and heteronuclear cases with mono- and disubstitution. There is no significant correlation observed between  $q_{\text{H}}$  and  $E_{\text{HB}}$ , in the weak hydrogen bonding region. In the moderate-to-strong hydrogen bond regime, i.e.,  $9 \text{ kcal/mol} < E_{\text{HB}} < 14 \text{ kcal/mol}$ , the correlation is system dependent, i.e., the extent of correlation changes with the type of donor atom being N or O (for example, in the  $\text{O}-\text{H}\cdots\text{O}$  case, the correlation value is 0.94 for  $R_2 = \text{H}$  and  $R_1 = \text{H}, \text{CH}_3, \text{Cl}, \text{NH}_2, \text{OH}$ ) or with the type of the substituent and there is a positive slope, meaning that upon increasing charge on the hydrogen atom the hydrogen bond energy also increases. However, when it comes to the strong hydrogen bond region, where  $E_{\text{HB}} > 15 \text{ kcal/mol}$ , an inverse proportionality has been observed in some cases, depending on the substituent neighboring the proton-bearing oxygen atom, i.e., when  $R_1 = \text{CF}_3, \text{COCl}, \text{NO}_2$  or  $R_2 = \text{NH}_2, \text{N}(\text{CH}_3)_2, \text{OH}$ , etc. For example, in the case of  $R_1 = \text{CF}_3, \text{COCl}$  and  $R_2 = \text{NH}_2, \text{N}(\text{CH}_3)_2$  the correlation value is equal to 1.00. That is, the hydrogen bond energy decreases as the charge on the hydrogen atom increases. This is an interesting situation because a positive slope would actually be expected in the electrostatic model of hydrogen bonding. Therefore, this negative slope can be interpreted as a clear indication of diminishing importance of hardness related properties that are also intuitively related to the electrostatics in the strong regime.

As a further estimate of the diminishing importance of hard-hard or electrostatic interactions the molecular electrostatic potential (MEP) values are considered. The values for the MEP are calculated at a distance of 2 Å from the acceptor and donor atoms in their isolated forms, i.e., in the absence of any hydrogen bonding interactions as in the non hydrogen bonded cT or tT conformers of Figure 2. When the molecules are considered altogether, a general trend of decrease in  $E_{\text{HB}}$  as the MEP of the donor increases in the moderate and strong hydrogen bond region has been observed (Figure 6). This is complementary to the information obtained from hydrogen atom NPA charges. The donor part can be simplified into an acid of the form  $\text{A}-\text{H}$ . If the acidity of  $\text{A}-\text{H}$  increases, then a stronger hydrogen bond will be formed since  $\text{A}^-$  will be less basic and will be more enthusiastic for giving away the proton to a base :B in the neighborhood, which is the acceptor atom. On the other hand, when the basicity of A decreases, then MEP in the neighborhood

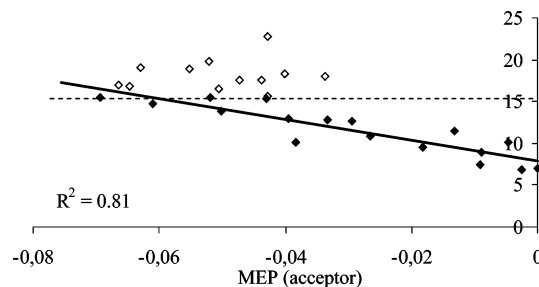


**Figure 7.** Hydrogen bond energy ( $E_{\text{HB}}$ ) versus MEP of acceptor atom in the moderate and moderate-to-strong hydrogen bond region for  $\text{O}-\text{H}\cdots\text{O}$  type of hydrogen bonds. (Unfilled bullets above the plateau are not incorporated in the regression.)

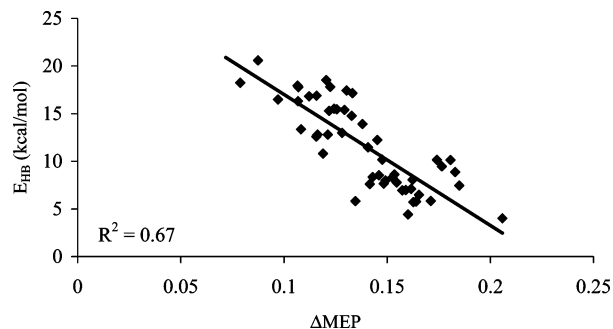


**Figure 8.** Hydrogen bond energy ( $E_{\text{HB}}$ ) versus  $\Delta\text{MEP}$  for 52 structures in all hydrogen bonding regimes.

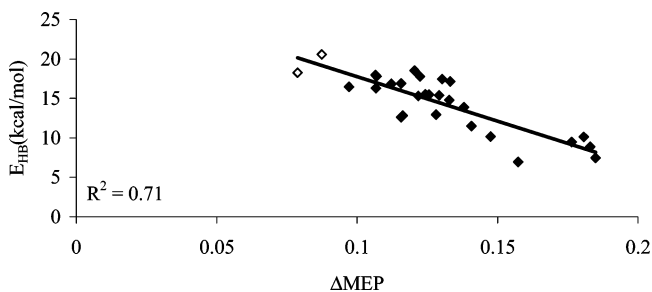


**Figure 9.** Hydrogen bond energy ( $E_{\text{HB}}$ ) versus  $\Delta\text{MEP}$  for  $\text{O}-\text{H}\cdots\text{O}$  type of hydrogen bonds.

of A will be less negative. In the same manner, a more negative MEP value will correspond to a more basic A and a weaker hydrogen bond between A and B (Figure 6). There has been a stronger dependence on the type of system under consideration when considering the correlation with the MEP of the acceptor. Therefore, homonuclear and heteronuclear bonds are examined separately. The best correlation has been obtained for the  $\text{O}-\text{H}\cdots\text{O}$  type in the moderate and moderate-to-strong hydrogen bond region, whereas there was no correlation for the same case in the strong hydrogen bond region, which is above “MEP of acceptor plateau” (Figure 7).

The trends in Figures 6 and 7 resemble the trends with PA [donor] and PA [acceptor] situations mentioned before. Therefore, a kind of “MEP matching” has been proposed in a manner similar to PA matching but with even a better overall correlation (Figure 8).

When the structures have been partitioned as homonuclear and heteronuclear hydrogen bonds, the best and poorest correlations were found for the  $\text{O}-\text{H}\cdots\text{O}$  (Figure 9) and  $\text{N}-\text{H}\cdots\text{N}$  cases, respectively, with the same general trend of increasing  $E_{\text{HB}}$  with decreasing  $\Delta\text{MEP}$  values. It can be concluded that  $\Delta\text{MEP}$  might be used as a reactivity descriptor for determining hydrogen bonding trends, especially for molecules in the moderate and moderate-to-strong hydrogen bonding regions.

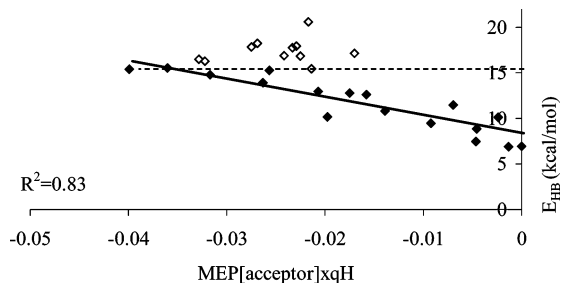


**Figure 10.** Hydrogen bond energy ( $E_{\text{HB}}$ ) versus  $\text{MEP}[\text{acceptor}] \times q\text{H}$  in the moderate and moderate-to-strong hydrogen bond region for O–H···O type of hydrogen bonds. (The horizontal line delineates the region of strong hydrogen bonding. Unfilled bullets above this plateau are not incorporated in the regression.)

However, as in the case of  $\Delta\text{PA}$ , there is a slight deviation from the general trend in the strong hydrogen bonding regime. This might be explained by the condition of reaching a “saturation” point or a plateau, especially for the MEP of acceptor atom, at a certain value of hydrogen bond energy (Figure 7). After this point, there is not much change in the MEP of the acceptor and, therefore, even with some little increase in the MEP of donor, the slope will change and might even become positive, changing even the trend. Finally, it can be concluded that in the strong hydrogen bond region  $\Delta\text{MEP}$  might not “work” because electrostatics fails to dominate or govern the interaction energy.

Alternatively,  $\text{MEP}[\text{acceptor}] \times q\text{H}$  values have been examined in order to have a different perspective on the strength of the electrostatic interactions. Again, the correlations have been system dependent and very poor in the cases where the N atom is the proton-donor atom in both the homonuclear and heteronuclear hydrogen bonds. The correlations have improved in the homonuclear O–H···O and heteronuclear N···H–O cases where the O atom is the proton-donating atom, especially in the moderate and moderate-to-strong hydrogen bonding region. The correlation was most plausible for the O–H···O type of bonding in this particular regime when  $E_{\text{HB}} < 15$  kcal/mol ( $R^2 = 0.83$ ). Figure 10 shows the contribution of electrostatic interactions to the hydrogen bond energy up to the strong hydrogen bond limit and, thereby, maps the area where the simple electrostatic model (SEM) is effective. There was no correlation at all with hydrogen bond energy and  $\text{MEP}[\text{acceptor}] \times q\text{H}$  parameters in the strong hydrogen bonding regime. Inclusion of this region into the graph, shown as unfilled bullets, in Figure 10, drops the correlation value to 0.59. Also, a plateau-like structure is observed when approaching the strong hydrogen bond region that can be interpreted as the “region of saturation” and above which no correlation is found anymore.

In the same manner, it has been attempted to correlate local hardness,  $\eta(\bar{r})$ , values of acceptor and donor atoms and the difference between them to hydrogen bond energies.  $\eta(\bar{r})$  values were evaluated starting from eq 7. The results have been system dependent as in the previous cases. The correlation levels were not promising for the weak regions of the heteronuclear hydrogen bonded structures. For the moderate regimes of homonuclear N–H···N and O–H···O types, local hardness of the donor atom shows a better correlation with the hydrogen bonding energy than the acceptor but still with  $R^2$  less than 0.70. Hydrogen bonding energy increased with increasing local hardness of the donor whereas the trend was opposite for the  $E_{\text{HB}}$  versus local hardness of the acceptor plot.  $\Delta\eta(\bar{r})$  values, which correspond to the difference in local hardness between acceptor and donor or  $\Delta\eta(\bar{r}) = \eta(\bar{r})_{\text{donor}} - \eta(\bar{r})_{\text{acceptor}}$ , have been considered separately within the N–H···N and O–H···O

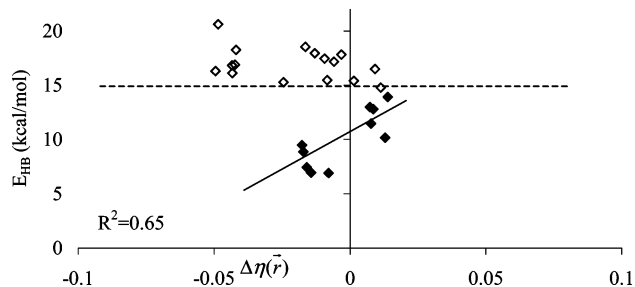


**Figure 11.** Hydrogen bond energy ( $E_{\text{HB}}$ ) versus  $\Delta\eta(\bar{r})$  (donor–acceptor) for O–H···O type of hydrogen bonds. (The horizontal line delineates the region of strong hydrogen bonding. Unfilled bullets above this plateau are not incorporated in the regression.)

subgroups since there was not an overall correlation when all of the structures were taken account. In the moderate regions, the hydrogen bonding energy increased with increasing  $\Delta\eta(\bar{r})$ , with poor correlations, however ( $R^2$  in the range 0.65–0.69). Figure 11 represents the change in hydrogen bonding energy with changing  $\Delta\eta(\bar{r})$  values for the strong hydrogen bonding regime.

When MEP and  $\eta(\bar{r})$  correlations are compared, it can be concluded that MEP is a better descriptor than  $\eta(\bar{r})$  for defining the electrostatic interactions in hydrogen bond formation. The correlation between  $\Delta\text{MEP}$  and  $\Delta\eta(\bar{r})$  is not as promising as the case with  $\Delta pK_a$  and  $\Delta\text{PA}$  and, for example, for the O–H···O system, it is best when  $E_{\text{HB}} < 15$  kcal/mol ( $R^2 = 0.73$ ). On the other hand, the correlation is not only decreased to a poor value ( $R^2 = 0.52$ ) but also inverted for the strong hydrogen bond regime, probably due to the effects of the plateau in Figure 11.

**Softness Role.** Soft–soft interactions within the present systems have been investigated in order to gain insight into the covalent nature of the hydrogen bonding. For that purpose, local softness values for radical attack,  $s^0$ , have been calculated both for the acceptor and for the donor atoms. Somehow similar to the situation observed with the proton affinity and MEP, the correlations between the hydrogen bonding energies and local softness values have been valuable only for closely related systems. Even though there was not observed an overall correlation for the complete set of the systems studied in all hydrogen bonding regimes, trends have become distinct by examining the homonuclear (N–H···N and O–H···O) and heteronuclear (N–H···O and N···H–O) cases separately. In addition to this fragmentation, correlations have been improved, in the strong hydrogen bonding regime especially, by changing  $R_2$  of Figure 1 for a certain  $R_1$  substituent and vice versa. Only weak or moderate correlations depending on the substitution pattern have been observed for the cases N–H···N and N–H···O, i.e., when the N atom is the proton donor, in the weak and moderate hydrogen-bonding regime. The correlation values improve for the cases N···H–O and O···H–O, i.e., when the O atom is the proton donor, in the moderate and strong hydrogen bonding regimes. For example, in the former heteronuclear case, hydrogen bonding energy increases with local softness of the donor with a correlation of 0.94, for  $R_2 = \text{H}$  and  $R_1 = \text{Cl, F, NH}_2, \text{NO}_2, \text{OH}$  substitution pattern of Figure 1, whereas the correlation is weaker for the acceptor ( $R^2 = 0.38$ , which increases to 0.91 by the exclusion of  $R_1 = \text{NH}_2$ ). For the latter homonuclear case, many groups or “families” of closely related systems have been formed with good correlations of hydrogen bonding energy and local softness of the acceptor or donor atoms.

For example, Figure 12 shows the change in hydrogen bonding energy with a change in the acceptor’s local softness

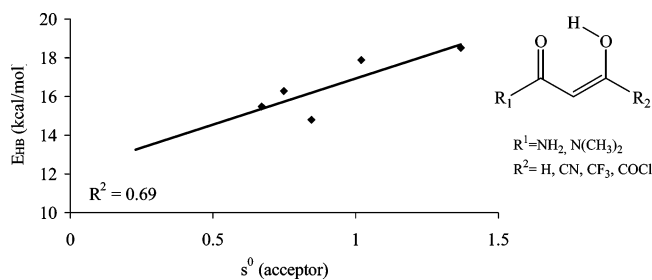


**Figure 12.**  $E_{\text{HB}}$  (kcal/mol) versus local softness of acceptor for  $\text{NR}_2$  family

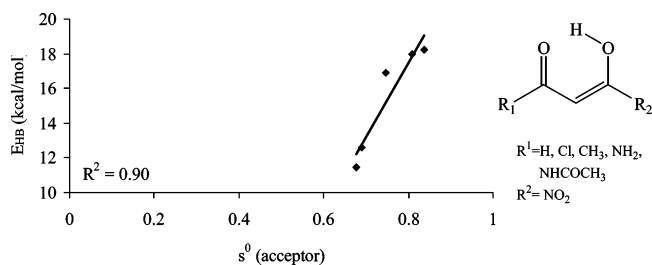


**Figure 13.**  $E_{\text{HB}}$  (kcal/mol) versus local softness of donor for  $\text{NO}_2$  family.

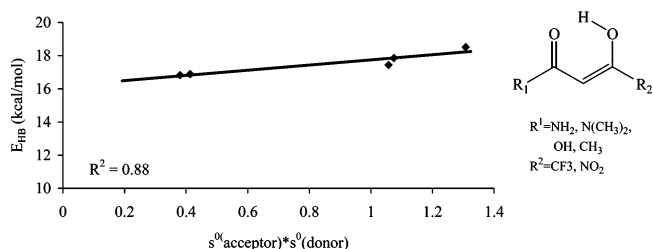
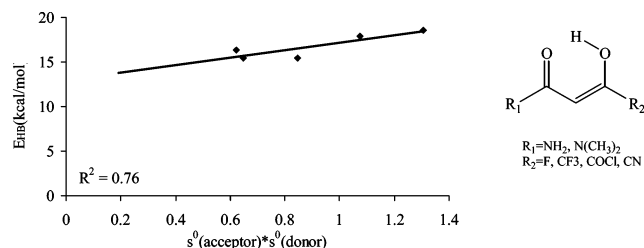


**Figure 14.** Combined effects of the local softness values of the acceptor and donor atoms on hydrogen bonding energy.

value for the “ $\text{NR}_2$  family” of the  $\text{O}-\text{H}\cdots\text{O}$  type of bonds. The correlation increases to 0.91 when  $E_{\text{HB}} > 15$  kcal/mol.

Figure 13 shows the change in hydrogen bonding energy with a change in the donor’s local softness value for the “ $\text{NO}_2$  family” of the  $\text{O}-\text{H}\cdots\text{O}$  type of bonds. The correlations are 0.76 for  $\text{COCl}$ , 0.99 for  $\text{NH}_2$ , and 0.94 for  $\text{NR}_2$  groups (i.e.,  $\text{R}_2 = \text{COCl}$  for different  $\text{R}_1$ s,  $\text{R}_1 = \text{NH}_2$  and  $\text{NR}_2$  for different  $\text{R}_2$ s, respectively).

Since both donor and acceptor local softness values have been increasing with increasing  $E_{\text{HB}}$ , it was not possible to derive a  $\Delta\text{PA}$ -match-like correlation in the strong hydrogen bond regime. On the other hand, the plot of  $E_{\text{HB}}$  versus  $s^0[\text{acceptor}] \times s^0[\text{donor}]$  might show the combined effect of the softness values in order to determine the extent of soft–soft interactions, and it has been useful for some closely related systems in the strong hydrogen bonding regime where hydrogen bond energy increases with increasing contribution of the local softness values of the acceptor and donor atoms (Figure 14). This regime actually scans the area above “the region of saturation” of Figure 10. Indeed, a second-order effect can be discerned here, which enters the picture when the first-order electrostatic effects are

saturated and then becomes the discriminating factor of hydrogen bonding strength. The appearance and dominance of this second-order effect can be interpreted through the strong polarization of the acceptor and donor atoms. It should also be noted that a special approach to *softness matching*<sup>19,34</sup> has been adapted in this study. According to this method, which was originally derived from the Pearson’s hard and soft acids and bases (HSAB) principle,<sup>23</sup> the most favorable interaction between the sites A and B occurs when  $\Delta s = s_A - s_B = 0$ , or, in other words, when  $s_A = s_B$ . However, in the present strong hydrogen bonded systems, the spirit of softness matching has changed from looking for a minimal  $\Delta s$  value to a maximal value of the product  $s_A \times s_B$ . This procedure can be justified in the following way: the local version of the HSAB principle states that soft–soft interactions occur preferentially between sites of the same softness. However, if both values are small at the local level, one can hardly expect a matching to represent an ideal situation for soft–soft interactions. On the other hand, the product of local softness values combines the idea that the difference should be small but at the same time the individual values should be large and, therefore, is a better approach to the soft–soft interactions in the present systems.

Since there is a one-to-one correspondence between covalent and soft interactions, the local-softness-related trends obtained in the strong hydrogen bonding region might be promising as a sign of the covalent character introduced, supporting the electrostatic–covalent hydrogen bond model (ECHBM).

## Conclusions

The purpose of this study was to gain a picture of the electrostatic versus covalent aspect of hydrogen bonding, not in the wave function context where valence bond theory could be used but rather in a conceptual density functional theory context. As a part of this task, high and uniform level calculations on hydrogen bond energy and related quantities such as  $\text{PA}$ ,  $\text{pK}_a$ , and DFT reactivity descriptors such as local hardness and local softness have been presented altogether here for the first time. The hydrogen bond energy versus  $\Delta\text{PA}/\Delta\text{pK}_a$  relationship has been regained for systems studied by Gilli et al. In the area of conceptual DFT, it has been observed that hard–hard interactions, which are electrostatic interactions in nature, can be used to rationalize hydrogen bond energies up to around 15 kcal/mol. In the strong hydrogen bond regime, especially when  $E_{\text{HB}} > 15$  kcal/mol, deviations have been corrected by invoking softness related interactions. It is clear that in the low and mid strong region electrostatics is dominating but that in the high energy region, where a saturation of electrostatic effects seems to occur, softness, linked to covalency, enters the picture and makes the difference. So, our study illustrates the electrostatic versus covalent aspect of hydrogen bonding, not in a wave function context (valence bond theory) but in a conceptual DFT context. Local DFT type descriptors have been shown to be able to systematize and interpret stability data. Use of these descriptors for the study of the intermolecular hydrogen bonds is planned as future work.

**Acknowledgment.** A.S.Ö. gratefully acknowledges the NATO-A2 grant provided by The Scientific and Technological Research Council of Turkey (TUBITAK-BAYG) supporting her visit to VUB. A.S.Ö. is also thankful to her friends at VUB, G. Roos, P. Mignon, and S. Loverix, for the friendship and support they have provided during her stay in Brussels.

## References and Notes

- (1) Jeffrey, G. A. *An Introduction to Hydrogen Bonding*; Oxford University Press: New York, 1997.



- (2) Gilli, G.; Gilli, P. *J. Mol. Struct.* **2000**, 552, 1.
- (3) Coulson, C. A. In *Hydrogen Bonding*; Hadzi, D., Ed.; Pergamon Press: New York, 1959.
- (4) (a) Morokuma, K. *J. Chem. Phys.* **1971**, 55, 1236. (b) Kitaura, K.; Morokuma, K. *Int. J. Quantum Chem.* **1976**, 10, 325.
- (5) Stevens, E. D.; Lehmann, M. S.; Coppens, P. *J. Am. Chem. Soc.* **1977**, 99, 2829.
- (6) Pimentel, G. C. *J. Chem. Phys.* **1951**, 19, 446.
- (7) Reid, C. *J. Chem. Phys.* **1959**, 30, 182.
- (8) Kollman, P. A.; Allen, L. C. *J. Am. Chem. Soc.* **1970**, 92, 6101.
- (9) Gilli, G.; Bellucci, F.; Ferretti, V.; Bertolasi, V. *J. Am. Chem. Soc.* **1989**, 111, 1023.
- (10) Gilli, P.; Bertolasi, V.; Ferretti, V.; Gili, G. *J. Am. Chem. Soc.* **1994**, 116, 909.
- (11) Gilli, P.; Bertolasi, V.; Ferretti, V.; Gilli, G. *J. Am. Chem. Soc.* **2000**, 122, 10405.
- (12) Gilli, P.; Bertolasi, V.; Pretto, L.; Lycka, A.; Gilli, G. *J. Am. Chem. Soc.* **2002**, 124, 13554.
- (13) Gilli, P.; Bertolasi, V.; Pretto, L.; Ferretti, V.; Gilli, G. *J. Am. Chem. Soc.* **2004**, 126, 3845.
- (14) (a) Meot-Ner (Mautner), M. J.; *J. Am. Chem. Soc.* **1984**, 106, 1257. (b) Meot-Ner (Mautner), M. J. *Chem. Rev.* **2005**, 105, 213.
- (15) Zeegers-Huyskens, T. *J. Org. Chem.* **1999**, 64, 4946.
- (16) Chandra, A. K.; Zeegers-Huyskens, T. *J. Mol. Struct.* **2004**, 706, 75–83.
- (17) Chandra, A. K.; Nguyen, M. T.; Uchimaru, T.; Zeegers-Huyskens, T. *J. Phys. Chem. A* **1999**, 103, 8853.
- (18) Parr, R. G.; Yang, W. *Density-Functional Theory of Atoms and Molecules*; Oxford University Press: New York, 1989.
- (19) Geerlings, P.; De Proft, F.; Langenaeker, W. *Chem. Rev.* **2003**, 103, 1793.
- (20) Chermette, H. *J. Comput. Chem.* **1999**, 20, 129.
- (21) Parr, R. G.; Donnelly, R. A.; Levy, M.; Palke, W. E. *J. Chem. Phys.* **1978**, 68, 3801.
- (22) Kohn, W.; Becke, A. D.; Parr, R. G. *J. Phys. Chem.*, **1996**, 100, 12974.
- (23) (a) Pearson, R. G. *J. Chem. Educ.* **1968**, 45, 981. (b) Parr, R. G.; Pearson, R. G. *J. Am. Chem. Soc.* **1983**, 105, 7512. (c) Pearson, R. G. *J. Chem. Educ.* **1987**, 64, 561. (d) Pearson, R. G. *J. Chem. Educ.* **1999**, 76, 267.
- (24) Sanderson, R. T. *Science* **1951**, 114, 670.
- (25) (a) De Proft, F.; Amira, S.; Choho, K.; Geerlings, P. *J. Phys. Chem.* **1994**, 98, 5227. (b) De Proft, F.; Langenaeker, W.; Geerlings, P. *Tetrahedron* **1995**, 51, 4021. (c) Choho, K.; Van Lier, G.; Van de Woude, G.; Geerlings, P. *J. Chem. Soc., Perkin Trans. 2* **1996**, 1723.
- (26) (a) Langenaeker, W.; Demel, K.; Geerlings, P. *J. Mol. Struct. (THEOCHEM)* **1992**, 259, 317. (b) Le, T. N.; Nguyen, T. L.; De Proft, F.; Chandra, A. K.; Geerlings, P.; Nguyen, M. T. *J. Chem. Soc., Perkin Trans. 2* **1999**, 1249. (c) Nguyen, L. T.; Le, T. N.; De Proft, F.; Chandra, A. K.; Langenaeker, W.; Nguyen, M. T.; Geerlings, P. *J. Am. Chem. Soc.* **1999**, 121, 5992.
- (27) (a) Vivas-Reyes, R.; De Proft, F.; Geerlings, P.; Biesemans, M.; Willem, R.; Ribot, F.; Sanchez, C. *New J. Chem.* **2002**, 26, 1108. (b) Vivas-Reyes, R.; De Proft, F.; Biesemans, M.; Willem, R.; Geerlings, P. *Eur. J. Inorg. Chem.* **2003**, 1315. (c) De Proft, F.; Vivas-Reyes, R.; Biesemans, M.; Willem, R.; Martin, J. M. L.; Geerlings, P. *Eur. J. Inorg. Chem.* **2003**, 3803.
- (28) (a) Berkowitz, M.; Ghosh, S. K.; Parr, R. G. *J. Am. Chem. Soc.* **1985**, 107, 6811. (b) Ghosh, S. K. *Chem. Phys. Lett.* **1990**, 172, 77. (c) Harbola, M. K.; Chattaraj, P. K.; Parr, R. G. *Isr. J. Chem.* **1991**, 31, 395. (d) Langenaeker, W.; De Proft, F.; Geerlings, P. *J. Phys. Chem.* **1995**, 99, 6424.
- (29) Hocquet, A.; Toro-Labbé, A.; Chermette, H. *J. Mol. Struct. (THEOCHEM)* **2004**, 686, 213.
- (30) Geerlings, P.; Vos, A. M.; Schoonheydt, R. A. *J. Mol. Struct. (THEOCHEM)*, in press.
- (31) Parr, R. G.; Yang, W. *J. Am. Chem. Soc.* **1984**, 106, 4049.
- (32) (a) McAllister, M. A. *J. Mol. Struct. (THEOCHEM)* **1998**, 427, 39. (b) Pan, Y.; McAllister, M. A. *J. Mol. Struct. (THEOCHEM)* **1998**, 427, 221.
- (33) Frisch, M. J.; Trucks, G. W.; Schlegel, H. B.; Scuseria, G. E.; Robb, M. A.; Cheeseman, J. R.; Montgomery, J. A., Jr.; Vreven, T.; Kudin, K. N.; Burant, J. C.; Millam, J. M.; Iyengar, S. S.; Tomasi, J.; Barone, V.; Mennucci, B.; Cossi, M.; Scalmani, G.; Rega, N.; Petersson, G. A.; Nakatsuji, H.; Hada, M.; Ehara, M.; Toyota, K.; Fukuda, R.; Hasegawa, J.; Ishida, M.; Nakajima, T.; Honda, Y.; Kitao, O.; Nakai, H.; Klene, M.; Li, X.; Knox, J. E.; Hratchian, H. P.; Cross, J. B.; Adamo, C.; Jaramillo, J.; Gomperts, R.; Stratmann, R. E.; Yazyev, O.; Austin, A. J.; Cammi, R.; Pomelli, C.; Ochterski, J. W.; Ayala, P. Y.; Morokuma, K.; Voth, G. A.; Salvador, P.; Dannenberg, J. J.; Zakrzewski, V. G.; Dapprich, S.; Daniels, A. D.; Strain, M. C.; Farkas, O.; Malick, D. K.; Rabuck, A. D.; Raghavachari, K.; Foresman, J. B.; Ortiz, J. V.; Cui, Q.; Baboul, A. G.; Clifford, S.; Cioslowski, J.; Stefanov, B. B.; Liu, G.; Liashenko, A.; Piskorz, P.; Komaromi, I.; Martin, R. L.; Fox, D. J.; Keith, T.; Al-Laham, M. A.; Peng, C. Y.; Nanayakkara, A.; Challacombe, M.; Gill, P. M. W.; Johnson, B.; Chen, W.; Wong, M. W.; Gonzalez, C.; Pople, J. A. *Gaussian 03*, revision B.03; Gaussian, Inc.: Pittsburgh, PA, 2003.
- (34) Geerlings, P.; De Proft, F. *Int. J. Quantum Chem.* **2000**, 80, 227.